Lab on a Chip

Accepted Manuscript

This is an *Accepted Manuscript*, which has been through the Royal Society of Chemistry peer review process and has been accepted for publication.

Accepted Manuscripts are published online shortly after acceptance, before technical editing, formatting and proof reading. Using this free service, authors can make their results available to the community, in citable form, before we publish the edited article. We will replace this *Accepted Manuscript* with the edited and formatted *Advance Article* as soon as it is available.

You can find more information about *Accepted Manuscripts* in the Information for Authors.

Please note that technical editing may introduce minor changes to the text and/or graphics, which may alter content. The journal's standard Terms & Conditions and the Ethical guidelines still apply. In no event shall the Royal Society of Chemistry be held responsible for any errors or omissions in this *Accepted Manuscript* or any consequences arising from the use of any information it contains.

ROYAL SOCIETY OF CHEMISTRY

www.rsc.org/loc

A versatile valving toolkit for automating fluidic operations in paper microfluidic devices

Bhushan J. Toley, Jessica A. Wang, Mayuri Gupta, Joshua R. Buser, Lisa K. Lafleur, Barry R. Lutz, Elain Fu†, Paul Yager

Department of Bioengineering
University of Washington
Seattle, WA 98195-5061

† E.F.: School of Chemical, Biological, and Environmental Engineering
Oregon State University
Corvallis, OR 97331

Running Title: Paper microfluidic valving and automation toolkit

Keywords: Point-of-care diagnostics, automation, actuators, system integration, 2DPN, wicking flow

Correspondence to:
Bhushan J. Toley
Department of Bioengineering
University of Washington
Box 355061, Foege N107
3720 15th Ave NE
Seattle, WA 98195-5061
Phone: 206-543-8063
Email: btoley@uw.edu

Lab on a Chip Accepted Manuscript

Table of Contents Entry

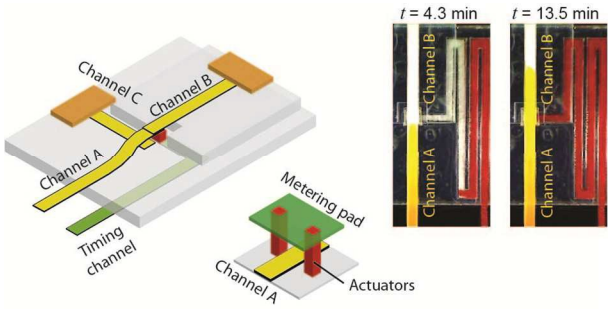

A versatile, powerless, valving and automation toolkit for paper microfluidic devices that uses absorbent expanding elements as actuators is presented.

Lab on a Chip Accepted Manuscript

Abstract

Failure to utilize valving and automation techniques has restricted the complexity of fluidic operations that can be performed in paper microfluidic devices. We developed a toolkit of paper microfluidic valves and methods for automatic valve actuation using movable paper strips and fluid-triggered expanding elements. To the best of our knowledge, this is the first functional demonstration of this valving strategy in paper microfluidics. After introduction of fluids on devices, valves can actuate automatically a) after a certain period of time, or b) after the passage of a certain volume of fluid. Timing of valve actuation can be tuned with greater than 8.5% accuracy by changing lengths of timing wicks, and we present timed on-valves, off-valves, and diversion (channel-switching) valves. The actuators require ~30 µl fluid to actuate and the time required to switch from one state to another ranges from ~5 s for short to ~50s for longer wicks. For volume-metered actuation, the size of a metering pad can be adjusted to tune actuation volume, and we present two methods – both methods can achieve greater than 9% accuracy. Finally, we demonstrate the use of these valves in a device that conducts a multi-step assay for the detection of the malaria protein P*f*HRP2. Although slightly more complex than devices that do not have moving parts, this valving and automation toolkit considerably expands the capabilities of paper microfluidic devices. Components of this toolkit can be used to conduct arbitrarily complex, multi-step fluidic operations on paper-based devices, as demonstrated in the malaria assay device.

Lab on a Chip Accepted Manuscript

Introduction

Paper microfluidic devices enable the controlled movement of microliter quantities of fluids without pumps. Fluids in these devices move by wicking action, i.e., capillary forces generated by the substrate porous materials. Because they do not require electricity or permanent instruments to operate, paper microfluidic devices present a promising platform for designing portable, low-cost, technically simple biochemical sensors[1–4]. They provide an opportunity to conduct healthcare diagnostic assays in remote and low-resource settings, where constant electric supply and maintenance of sophisticated instruments is a challenge[5]. Several paper-based devices have been designed for conducting colorimetric analytical chemistries[6–10] and lateral flow immunoassays[11–14]. The capabilities of paper microfluidics were enhanced by two major developments in the field – μPADs (microfluidic paper-based analytical devices) and 2DPNs (two-dimensional paper networks). μPADs, introduced by the Whitesides group in 2008, are 2D and 3D paper devices that distribute fluids from a common source to multiple detection zones and can be used for conducting multiplexed colorimetric assays[1,2,15,16]. 2DPNs, introduced by our group in 2010, can be used to flow multiple fluids sequentially to a detection zone and enable conducting highly sensitive, signal-enhanced immunoassays in paper-based devices, thus transcending the capabilities of conventional lateral flow immunoassays[17–23] (Here the term 'paper' is broadly used to represent porous materials, including nitrocellulose.)

A major milestone in the development of any microfluidic platform will be when it can enable conducting a complete 'sample-in-answer-out' (SIAO) type diagnostic test in a portable device operable by an untrained user. SIAO tests typically involve multiple steps to carry out processes such as sample preparation, assay chemistry, and colorimetric detection. The flow control and

Lab on a Chip Accepted Manuscript

automation capabilities of paper microfluidic devices are currently limited and such multi-step SIAO assays have not yet been conducted. As the flow-control capabilities of paper microfluidic devices improve, more complex, multi-step assays can be conducted. There is dire need of such low-cost technologies for conducting diagnostic tests in limited resource settings[24]. Currently, automatic multistep tests can only be conducted in expensive instruments, usually only available in sophisticated laboratories.

Valves are fundamental for enhancing the fluidic capabilities of any microfluidic platform. In paper microfluidic devices, valving is a challenge because valves must operate in absence of instrumented controllers and actuators. Several innovative strategies have been developed for paper microfluidic valving. Here, we refer to 'valves' as any method that can be used to control the flow rates of fluids in paper devices. Valves developed for paper microfluidics can be broadly classified into three categories based on the method used to control flow rates: a) those that use device geometry alone, b) those that make use of chemicals in the flow path, and c) those that use mechanical means to connect or disconnect channels. A brief review of these valving methods is presented next.

The simplest geometry-based flow control strategy is changing the width of channels[17,18,22]. Another method is changing the shape of a downstream wicking region[25]. Geometry-based methods of shutting flow off after a programmed volume of fluid flow have been developed. One method used source pads of different sizes that released a fixed volume of fluid[19,23]. Another design used vertical paper legs of different lengths that disconnected from a fluid reservoir after passage of fixed fluid volumes[21]. Controlled flow-delay lines were created by using pads of

Lab on a Chip Accepted Manuscript

porous materials as shunts[26]. Valves in the second category make use of chemicals in the flow path to alter flow rates. Controlled delays in fluid flow were obtained by depositing different amounts of sugar on paper channels[27]. Solid sugar blocked flow and flow resumed after sugar dissolved. Complementary to this, controlled flow shut-off was demonstrated by using dissolvable sugar[28] and dissolvable polymeric[29] bridges. In both cases, fixed fluid volumes flowed across the sacrificial bridges. Paraffin wax was used in one demonstration to alter the rate of fluid flow from a source to multiple target regions on a paper device[30]. Chen et al. developed paper microfluidic diodes that made use of surfactant to bridge a hydrophobic gap in the flow path[31,32]. In another case, flow rate was controlled by electrowetting of a dielectric deposited on paper[33]. The third category of paper microfluidic valves involves mechanical means to connect or disconnect channels. Several of these require manual actuation[16,34–36]. In one design, valves were actuated by electromagnets in response to the arrival of fluid at a certain location on the device[37].

In this article, we present a new strategy of valving and programming automatic valve actuation in paper microfluidic devices and demonstrate how it can be used to design a SIAO protein detection device that can be operated by an untrained user. Although some aspects of the valving strategy were presented in patents published in the early 1990's[38–40], the work was apparently not needed for commercial lateral flow products at the time and was neither developed nor widely known in academia. Over the last few years, we have developed valving methods using a related strategy and have designed multiple functional valves. To the best of our knowledge, these are the first demonstrations of functional paper microfluidic valves using this strategy. The work described here was conducted in the context of two projects aimed at developing low-cost, rapid

Lab on a Chip Accepted Manuscript

and sensitive infectious disease diagnostics using paper: one based on nucleic acid amplification and the other based on protein binding. Both projects use the wicking action of paper-like materials to move fluids with minimum ancillary equipment and conduct SIAO-type multi-step diagnostic assays in devices that can be operated by untrained users. In contrast to most other valves that enable a single fluidic operation, we present an entire toolkit of paper microfluidic flow-control tools that can be used to design multiple types of valves, i.e., on-switches, off-switches, and flow-diversion switches. We also present a strategy to automatically actuate these valves after a chosen period of time or after the passage of a chosen volume of fluid. The valves fall under the category of mechanical actuation and use fluid-activated expansion of absorbent materials for actuation (expandable elements activated by pH of process fluids have previously been used for valving in conventional microfluidic devices[41,42]). The design of these valves and all devices presented in this article is motivated by previously developed 2DPN devices in our group. The primary difference compared to 2DPNs is that, whereas all channels in a 2DPN reside on a single plane and stay connected throughout a test, the channels of devices presented here are placed at different heights and connect or disconnect during the course of the test, which makes these devices three-dimensional. Three highly desirable characteristics of these valves are i) they do not require batteries or electricity to operate, ii) they do not introduce chemicals in the flow path, and iii) their actuation can be pre-programmed so that user intervention is not required. Because it enables automation of multiple types of valves using a common set of fabrication processes, this toolkit enhances the capabilities of paper microfluidic devices and enables conducting SIAO tests in paper microfluidic devices. It is noteworthy that the initial patents on this core technology have now expired and these valves are available for use by all.

Lab on a Chip Accepted Manuscript

Results and Discussion

Valving Concept and Classification of Valves and Actuation Methods

The fundamental mechanism of valving utilized here is the displacement of one end of paper channels causing connection or disconnection with other channels, triggered by the arrival of fluid at the actuators. Actuation can be automated by designing geometries that control the arrival of fluid to the actuators. Expandable absorbent materials, such as hydrogels, sponges, or other porous materials (such as cellulose) constitute one class of actuators. Ideal actuators would be those that expand reproducibly and fast, and have a high ratio of actuation displacement to volume of actuation fluid. Here, we tested two materials as actuators – compressed cellulose sponges and sodium polyacrylate (SP; a superabsorbent hydrogel used in diapers). We successfully built valves with both actuators. The expansion of compressed sponges was found to be faster and more reproducible than SP. All valves illustrated in this article use compressed sponges as actuators. For a comparison of the performance of sponges with SP, see Supporting Information Sections I and II.

The different types of valves presented here can be classified into two categories: those that can be programmed to actuate after a fixed period of time (branch A; Fig. 1) and those that can be programmed to actuate after the passage of a fixed volume of fluid (branch B; Fig. 1). These two types of valves use different fluid sources for actuation. Devices with timed valves contain a timing fluid that flows in the timing channels, which is isolated from the process fluid that flows in the flow channels. Timing is controlled by the shape and length of the timing channel. On the other hand, volume-metered valves are designed specifically to meter the flow of a process fluid.

Lab on a Chip Accepted Manuscript

This is achieved by diverting the process fluid to a metering pad, which is connected to actuators. These valves do not require a separate actuation fluid. Three types of timed valves are presented: on-switches, off-switches, and diversion-switches (branches A1, A2, and A3, respectively; Fig. 1). As illustrated in branches A1-A3 (Fig. 1), when actuated, on-switches start flow, off-switches stop flow, and diversion-switches divert flow from one channel to another. The most practical application of an active volume-metered valve is a diversion-switch (volume-metered off-switches such as dead-end channels and limited volume fluid sources can be constructed in passive devices; volume-metered on switches cannot be constructed because there must be fluid flow before valve actuation). Two different designs of volume-metered diversion switches are presented. As illustrated in branch B, Fig. 1, both methods divert fluid flow from flowing into a metering pad to flowing downstream in the device. In one method, a paper channel is displaced to disconnect from the metering pad (branch B1; Fig. 1), and in another method, the metering pad is displaced to disconnect from the paper channel (branch B2; Fig. 1).

Time-metered Valves

Three types of valves that can be programmed to actuate after a certain period of time were designed. The valves are demonstrated here in absence of programmed timing first, focusing on the valving mechanism. An on-switch (branch A1; Fig. 1) starts fluid flow when actuated. It consists of two collinear flow channels, channel A and channel B, placed at different heights with one end overlapping, but not touching (Fig. 2A). Channel A is a cantilever channel, permanently secured to the surface at its left end, placed at a lower height than channel B. There is no initial contact between the two channels. The right end of channel A is attached to an impermeable fluid barrier, which is attached to the surface over a square cavity. This bond is not

Lab on a Chip Accepted Manuscript

permanent; it breaks when the actuator expands. The purpose of the bond is to secure the end of channel A before valve actuation. The cavity contains a compressed sponge actuator (Fig. 2A). An actuation channel connects to the actuator from below (Fig. 2A). When the actuating fluid reaches the actuator, the actuator expands, lifts the right end of channel A, and establishes its contact with channel B (Fig. 2A; bottom panel). The impermeable barrier ensures that actuating fluid does not enter the flow channels.

We present one specific implementation of an on-switch in which channels A and B are made of 4.5 mm-wide plastic-backed nitrocellulose (Fig. 2B; Movie S1 in Supporting Information). The height difference between the channels is 1.5 mm, and they are oriented such that their nitrocellulose sides face each other. The actuation channel is also 4.5 mm wide and is composed of high permeability glass fiber. Glass fiber channels were selected over nitrocellulose or cellulose (filter paper) channels because they delivered fluid to the actuator faster, which enabled faster valve actuation. The actuator is a 4.5 mm square piece of compressed cellulose sponge, 2.3 mm tall, placed in a 5.6 mm square cavity, 2.5 mm deep. Channel A and the actuation channel were connected to fluid reservoirs. When a yellow process fluid (1 mg/ml solution of phenol red at pH 8) was introduced in channel A at time $t = 0$, it flowed toward the end of the channel until the channel was saturated (Fig. 2B; left panel). As long as the actuation channel was dry, the sponge remained compressed, and there was no further flow in the flow channels (Fig. 2B). Fig. 2C shows the speed of the fluid front as a function of time. The reduction of flow rate from 0 – 5 minutes is a characteristic of wet-out flow, during which, fluid is imbibed into paper channels, and is explained by the Lucas-Washburn equation[22,43–45], according to which the speed of the fluid front is related to time, t, as $t^{-0.5}$. In this example, channel A saturated at around 6 minutes

Lab on a Chip Accepted Manuscript

after introduction of the process fluid, at which time, the flow rate became zero (Fig. 2C; pink zone). The valve was held in this position for 5 minutes and then water was introduced in the actuation channel. The water reached the actuator at ~12.5 minutes and actuated the valve. Upon actuation, process fluid started flowing from channel A to channel B (Fig. 2B; right panel). The step change in flow rate after valve actuation is seen in Fig. 2C (transition from pink to green zone). The subsequent reduction in flow rate is due to wet-out flow (Fig. 2C; green zone). The actuators are fast and reproducible. The time required for the process fluid to enter channel B after the actuating fluid reached the actuator was 3 – 6 seconds (N=6). The average time required for the process fluid to flow 1 cm into channel B after actuating fluid reached the actuator was 1.9 minutes with a standard deviation of 9 seconds (coefficient of variation (CV) = 8%; N=6). This measurement excludes the variation in time required for the actuating fluid to flow through the actuation channel, thus, is a measure of the reproducibility of the actuator alone. Actuation time of these valves can be further reduced by reducing the size of the actuator, which will reduce the amount of fluid required for actuation. However, there is a lower limit on the size of the actuator below which the actuator may not generate enough force. While designing these valves, it must be ensured that an excess volume of actuation fluid is available because sponge actuators cease to expand if the supply of fluid is stopped prematurely.

The next type of valve is an off-switch (branch A2; Fig. 1), which stops fluid flow when actuated. It consists of two perpendicular channels, channel A (cantilever style) and channel B (Fig. 2D). The two channels are placed at the same level. Where they cross, channel A makes contact with channel B placed under it, and extends slightly over channel B (Fig. 2D). The overhanging section of channel A is attached to an impermeable fluid barrier, which is attached

Lab on a Chip Accepted Manuscript

to the surface over a square cavity containing the actuator (Fig. 2D). An actuation channel connects to the actuator from below. Upon actuation, the right end of channel A is lifted up and disconnected from channel B (Fig. 2D; bottom panel). Similar to the on-switch demonstrated above, an off-switch can be constructed with two plastic-backed channels of nitrocellulose with their nitrocellulose sides facing each other. However, in order to use an electrochemical band marking setup[18] to track fluid velocity over time, the top surface of channel A needed to be exposed. To satisfy this, in this implementation channel A was constructed of 4.5 mm wide unbacked nitrocellulose (Movie S2 in Supporting Information). All other materials and dimensions were identical to the on-switch example. When a yellow process fluid was introduced into channel A, it flowed through channel A into channel B (Fig. 2E; top panel). Flow was sustained by a cellulose wicking pad attached to the end of channel B (Fig. 2E). Fig. 2F shows the linear velocity of the fluid as a function of time as measured by tracking colored bands generated by the band-marking setup. The reduction in speed expected for Lucas-Washburn flow can be seen from 0 – 20 minutes (Fig. 2F; pink region). After ensuring sustained flow from channel A to channel B (Fig. 2F; pink zone), water was added to the glass fiber actuating channel at 19 minutes and reached the actuator at 20 minutes. Valve actuation stopped the flow of process fluid (Fig. 2E; bottom panel and Fig. 2F; green zone). In all 5 repetitions, the velocity in channel A dropped to below 10% of the velocity at the time of actuation within 4 minutes. The slow bleed of flow after valve actuation was caused by unsaturated zones (dead volume) in channel A downstream the region where it crossed channel B and occurred after the two channels had disconnected. An alternate design, in which, the overhanging part of channel A is eliminated by moving the actuator upstream the intersection of channels, can eliminate this dead

Lab on a Chip Accepted Manuscript

volume. The two channels can also be placed collinearly in this alternate design. However, we found that the design presented here facilitates better initial contact between channels.

A flow-diversion switch (branch A3; Fig. 1) is a combination of an on-switch and an off-switch and diverts fluid flow from one channel to another when actuated. It consists of three channels – a source channel A (cantilever style), and two sink channels, B and C (Fig. 2G). The design of this valve is identical to the off-switch, with the addition of a third channel, channel C (Fig. 2G). Expansion of the actuator causes channel A to disconnect from channel B and connect to channel C (Fig. 2G; bottom panel). Because channel A must make contact with both channel B placed under it, and with channel C placed above it, it is imperative that channel A be made of an unbacked material. In the example presented here, channel A is made of unbacked nitrocellulose, while channels B and C are made of plastic-backed nitrocellulose, oriented such that their nitrocellulose sides face channel A (Movie S3 in Supporting Information). All other materials and dimensions are identical to the off-switch example presented above. When a yellow process fluid was introduced in channel A, it flowed through channel A into channel B, but not into channel C (Fig. 2H; left panel). Water was then introduced into the actuation channel and reached the actuator at 20 minutes. After valve actuation, fluid stopped flowing into channel B and started flowing into channel C (Fig. 2H; right panel). A representative side view of the valve shows the displacement of channel A between positions 1 and 2 (Fig. 2I). The electrochemical band marking setup was used to measure fluid linear velocities. The step changes in flow rates between the two valve positions are seen in Fig. 2J – flow rate in channel B drops to zero and flow rate in channel C rises from zero to a higher rate on valve actuation.

Lab on a Chip Accepted Manuscript

Programming timing of valve actuation

Time-metered valves can be programmed to actuate automatically by controlling the time at which actuation fluid arrives at the actuators, for example, by using serpentine actuation channels of different lengths. In these designs, fluids are simultaneously introduced into the flow channels and the actuation channels of valves. This simplifies the operation of such devices to a single user step of initial fluid addition. Fig. 3A shows the automatic actuation of an on-switch with a pre-programmed time delay (Movie S4 in Supporting Information). The on-switch was constructed similar to the on-switch in Fig. 2B, but with a 2.9 mm-wide serpentine glass fiber actuation channel (Fig. 3A). A yellow fluid was introduced in a reservoir at time, t = 0, which initiated simultaneous flow of the fluid in channel A and the actuation channel (Fig. 3A; 1.5 min; note that the fluid appears darker in the thicker glass fiber channels compared to the nitrocellulose channels). Process fluid reached the end of channel A at 4.3 minutes and stopped (Fig. 3A; 4.3 min). Note that fluid flowed faster through the actuation channel compared to the flow channel because of different material properties, for example, higher permeability of the actuation channel compared to the flow channel. At 10 minutes, the actuation fluid reached the actuator (Fig. 3A; 10 min) and actuated the on-switch. At 13.5 minutes, the process fluid front can be seen in channel B (Fig. 3A; 13.5 min). In 5 replicates of this design, the on-switch actuated at a mean time, t = 10.2 minutes, with a standard deviation of 42 seconds (CV = 6.9%; N=5). Timed and reproducible valve actuation can thus be achieved. One implication of increasing the length or decreasing the width of actuation channels is that it increases the resistance imposed on the actuation fluid. This decreases the rate at which fluid is delivered to the actuators, which decreases the rate of their expansion. In these valves, the time required for fluid to enter channel B after the actuation fluid reached the actuators was in between 30 – 50

Lab on a Chip Accepted Manuscript

seconds, which was greater than 3 – 6 seconds for valves shown in Fig. 2B. Assuming an infinite supply of fluid, valve actuation time can be tuned by changing the length of actuation channels. In order to determine the tunability and reproducibility of timing that can be achieved using glass fiber actuation channels, the time, t_{delay}, required for fluid to flow through different lengths, L, of glass fiber actuation channels was measured (Fig. 3B). For five different channel designs, A-E (Fig. 3B), time delays ranging from 4.1 min to 23.8 min were achieved with better than 8.5% accuracy (except design A; Fig. 3B). See Supporting Information Section IV for details. Note that delays of the order of tens of minutes are necessary for conducting nucleic acid amplification assays[46] or protein detection assays requiring sequential delivery of multiple reagents[23], as we demonstrate below in an assay device.

This strategy of timing valve actuation can also be used to actuate multiple valves on a device sequentially. Fig. 3C shows a device with two on-switches actuated sequentially. It consists of three nitrocellulose flow channels, A, B, and C, placed at three different levels. On-switches lie between channel A and channel B (Valve 1; dotted rectangle; Fig. 3C), and between channel B and channel C (Valve 2; dotted rectangle; Fig. 3C). Because channel B makes contact with channel A placed below it and channel C placed above it, it was made of unbacked nitrocellulose. A 2.9 mm wide serpentine glass fiber actuation channel originated at the fluid reservoir, passed through Valve 1, and terminated at Valve 2 (Fig. 3C). Channel A and the actuation channel were inserted into a common fluid reservoir, which was filled with a yellow fluid at time, $t = 0$. Fig. 3C shows time-lapse images of the device in operation. At 9.3 minutes, the process fluid had reached the end of channel A but actuation fluid had not reached Valve 1. Valve 1 actuated at 15 minutes. At 17.6 minutes, actuation fluid had crossed Valve 1 and the

Lab on a Chip Accepted Manuscript

process fluid front was in channel B. At 37.5 minutes, process fluid had reached the end of channel B, but the actuating fluid had not reached Valve 2. Valve 2 actuated at 50.5 minutes. At 52.3 minutes, the process fluid front can be seen in channel C. This demonstrates controlled incubation and subsequent movement of fluid into different zones of a paper microfluidic device. This method can also be used to implement sequential delivery of fluids over a detection zone, as demonstrated in a protein detection assay below. This could be the basis of conducting automated multi-step biochemical assays in paper microfluidic devices.

Volume-metered valves

Volume-metered valves are useful for any washing operation where the important parameter is wash volume as opposed to reaction time. In such cases, these methods eliminate the need for using timing wicks. The particular application for which we developed these valves was in the context of a sample purification method in which the components of interest from a fixed sample volume are captured over a zone upstream from the valve, followed by elution of the captured components and their transport downstream from the valve, where they can be used for analysis. The sample fluid from which the components are captured is routed to a waste pad (the metering pad), which becomes disconnected from the system after valve actuation. Two types of volume-metered diversion switches are presented. The design of the first type of volume-metered switch (branch B1; Fig. 1) is similar to the time-metered switches presented above, i.e., it consists of two flow channels, A and B, placed at different heights (Fig. 4A). The valve actuates when one end of channel A is lifted up by the expansion of the actuator and makes contact with channel B (Fig. 4A). The primary difference compared to time-metered valves is that as opposed to using fluid in a separate actuating channel, volume-metered valves divert the process fluid towards the

Lab on a Chip Accepted Manuscript

actuator. A metering pad in between the flow channel and the actuator is used to meter the volume for valve actuation. Specifically, channel A makes contact with a metering pad placed under it near one end (Fig. 4A). The channel extends over the metering pad and connects to an impermeable fluid barrier, attached on top of a cavity containing the actuator (Fig. 4A). The bottom surfaces of the metering pad and the actuator are connected with a connector pad (Fig. 4A). Fluid introduced in channel A flows into the metering pad, then into the connector pad, and then into the actuator. Expansion of the actuator disconnects channel A from the metering pad and connects it with channel B (Fig. 4A; right panel).

A specific implementation of a volume-metered diversion switch with 1 cm wide nitrocellulose channels is presented here (Fig. 4B; Movie S5 in Supporting Information). Channel A was made of unbacked nitrocellulose because it must make contact with the metering pad and channel B placed on either sides. Channel B was made of plastic-backed nitrocellulose, and placed 2 mm above channel A. The metering pad and connector pads were 1 cm wide and made of cellulose. One of the requirements of this design is that the metering pad must be thick enough to protrude above the surface to contact channel A (Fig. 4A; left panel). The protrusion should be approximately equal to the thickness of the impermeable fluid barrier to ensure good contact with channel A (Fig. 4A; left panel). To attain the appropriate height, here, the thickness of the metering pad was adjusted by stacking 2.70 mm and 0.87 mm thick layers of cellulose. The actuator was made of 1 cm wide, 2.3 mm thick compressed cellulose sponge. The width, W, of the metering pad and the actuator (Fig. 4B) was used as a parameter to tune actuation volume. Two designs with $W = 0.5$ and 1 cm were fabricated. Time-lapse images of the valve with $W = 1$ cm are shown in Fig. 4B. Channel A was inserted into a fluid reservoir where a yellow fluid was

Lab on a Chip Accepted Manuscript

added at time $t = 0$. The electrochemical band marking setup was used to track fluid velocity. At $t = 4$ and 57 minutes, respectively, fluid flowed into channel A and into the metering pad (Fig. 4B). The valve actuated at $t = 60$ minutes. At $t = 65$ and 79 minutes, channel A had disconnected from the metering pad and fluid flowed into channel B and the cellulose wicking pad attached to it (Fig. 4B). The velocity through channel A for this valve was tracked as a function of time, t. After the initial decreases in velocity during wet out ($t < 10$ min), a nearly constant velocity was maintained in channel A while fluid flowed into the metering pad (Fig. 4C; pink zone). During actuation, the velocity into the metering pad decreased to zero over 4 minutes (Fig. 4C; rightmost region of pink zone). After actuation, flow entered channel B and a nearly constant velocity was maintained in the device (Fig. 4C; green zone). Finally, reproducibility and volume tunability of this valve are demonstrated. Volume before actuation was measured as area under the speed-time curve (Fig. 4C; pink zone). When W was changed from 1 cm to 0.5 cm, the volume required for valve actuation decreased to very close to half (Fig. 4D). For $W = 1$ and 0.5 cm, the mean actuation volumes were 197 µl (N=4) and 95 µl (N=5) with standard deviations of 7 and 14 µl, respectively.

The second type of volume-metered switch (branch B2; Fig. 1) is based on the displacement of metering pads and has fixed paper channels. The basic idea is shown schematically in a transverse view of this valve (Fig. 5A; left column). A metering pad with embedded expanding actuators is placed on top of a flow channel. The actuators extend out below the metering pad and are inserted in cavities on the surface. For this design, the properties of the metering pad relative to the flow channel must be such that the process fluid directly under the pad preferentially flows into the pad; there should be no flow in the channel downstream of where

Lab on a Chip Accepted Manuscript

the pad contacts it. This occurs when the capillary forces generated by the wicking pad, F_{pad}, are considerably higher than those generated by the channel, $F_{channel}$. For a detailed discussion of fluid flow in such assemblies, refer to Toley et al.[26]. If this condition is satisfied, after a certain volume of fluid accumulates in the metering pad, it reaches the actuators, which expand and lift the metering pad (Fig. 5A; left bottom panel), allowing fluid to flow downstream of the valve region. Flow diversion can thus occur using a single flow channel and one metering pad. When the flow channel is composed of nitrocellulose, a common material used in paper microfluidics, a modification to this basic design is necessary. Nitrocellulose generates large capillary forces and the necessary condition, $F_{pad} > F_{channel}$, is not satisfied for most combinations of pad materials and nitrocellulose. However, this problem can be resolved by inserting an adapter channel between two nitrocellulose channels, A and B, as shown in the lateral view of the schematic (Fig. 5A; right column). The adapter channel is made of glass fiber, generates lower capillary forces than nitrocellulose, and preferentially delivers fluid to a cellulose metering pad with little leakage downstream. Before valve actuation, fluid introduced into the nitrocellulose channel A flows into the metering pad through the adapter channel (Fig. 5A; top right panel). After actuation, fluid in channel A flows into channel B (Fig. 5A; bottom right panel).

A specific implementation of this volume-metered switch is shown in Fig. 5B (Movie S6 in Supporting Information). It consists of two 1 cm wide plastic-backed nitrocellulose channels, A and B, connected with a 1 cm wide glass fiber adapter channel. The metering pad was a 3 cm x 1.5 cm, 0.87 mm thick cellulose pad and had two 2.3 mm thick square sponge actuators of side 4.5 mm inserted within it (Fig. 5B). An adhesive Mylar layer was placed on top of the metering pad to hold the assembly together. A transparent block of poly (methyl methacrylate) (PMMA)

Lab on a Chip Accepted Manuscript

was attached on top of this as weight to ensure good contact between the metering pad and the adapter channel. Four PMMA support posts were built around the metering pad to constrain its horizontal motion during valve actuation. Channel A was connected to a fluid reservoir, in which yellow fluid was added at time, $t = 0$. At $t = 15$ min, fluid had flowed into the metering pad, through channel A and the adapter channel, but had not reached the sponge actuators (Fig. 5B). At $t = 38$ min, fluid had reached the actuators, the metering pad had lifted off, and fluid had flowed into channel B (Fig. 5B). Side view shows the compressed sponge before actuation and expanded sponge after actuation (Fig. 5B). Note that there was a darker fluid front downstream from the valve after actuation (Fig. 5B; $t = 38$ min; top view). We believe that this is a result of a) chromatographic separation caused by the adapter channel, and b) an increase in pH of the phenol red solution in the adapter channel (alternate adapter channel materials may eliminate this effect, but we have not tested other materials in this work). Flow rates (linear velocities) were measured in channel A (v_A) using the electrochemical band marking system and in channel B (v_B) by tracking the yellow fluid front. The flow rate into the metering pad, v_{pad}, was determined as $v_{pad} = v_A - v_B$. A plot of flow speed as a function of time shows initial reduction during wet out ($t < 5$ min; Fig. 5C) followed by sustained flow into the metering pad. Close to $t = 18$ min, flow rate into the metering pad started decreasing and flow rate in channel B started increasing slowly (Fig. 5C). At $t > 26$ min, flow rate into the metering pad became zero and flow rate in channel B increased to a steady rate (Fig. 5C; green zone). The mean volume that flowed into the metering pad before the valve actuated was 145 µl with a standard deviation of 12 µl (CV = 8.3%; N=3). The time between $t = 18 – 26$ minutes can be designated as the actuation period of this valve. Compared to volume-metered valves using cantilever channels (Fig. 4C), the actuation of this valve was less sharp and there was slight leakage into channel B before valve actuation was

Lab on a Chip Accepted Manuscript

complete (dotted rectangle; Fig. 5C). However, for applications where slight leakage can be tolerated, this valve provides a simpler design for volume metering because the flow channels are fixed. The PMMA weight may be replaced by a spring or a similar tension-mount assembly, which will make the design more compact. The actuation volume of this valve could be tuned by changing the geometry of the metering pad, the location of the actuators within the pad, and/or by stacking multiple metering pads on top of each other. Note that for volume-metering valves, sample viscosity may affect the time at which valves actuate, but volume for actuation is governed by the size of the metering pads and should be less sensitive to sample viscosity.

Demonstration of a protein detection assay

We demonstrate the use of sponge-based valves in a portable device for the detection of the malaria protein, *Plasmodium falciparum* histidine rich protein 2 (P*f*HRP2), using a signal amplified ELISA based on sequential delivery of reagents to a detection zone. The device has a footprint of 7.5 cm x 5.2 cm, smaller than a credit card, and is 2 cm tall at its highest point. All assay reagents are stored dry on the device. A top view of the device is shown in Fig. 6A. The base of the device is a 1.1 cm acrylic block with a fluid reservoir near one end. The test strip is made of 4-mm-wide plastic-backed nitrocellulose, porous side facing down. It is attached to a cellulose wicking pad at one end and to a sample inlet port on the other. Three on-switches, $V_{ON,1}$, $V_{ON,2}$, and $V_{ON,3}$, when actuated, connect dry reagent-containing glass fiber legs 1, 2, and 3, respectively, to the test strip. Dried reagents on these legs are rehydrated by a glass fiber feeder channel that is connected to the fluid reservoir. An off-switch, V_{OFF}, when actuated, disconnects the feeder channel from the three legs, converting them into limited volume fluid sources. A 2.5-mm-wide glass fiber timing wick, connected to the fluid reservoir, times the

Lab on a Chip Accepted Manuscript

actuation of the 4 switches on the device. The shape of the wick is shown in Fig. 6B. The wick splits at the point indicated by a green asterisk (*; Fig. 6B); one branch carries fluid to V_{OFF} and the other branch carries fluid to the three on-switches that are actuated in the order: $V_{ON,1}$, $V_{ON,2}$, and $V_{ON,3}$. Each on-switch actuation connects one leg to the test strip and delivers a reagent to the detection zone. The sequential actuation of valves results in sequential delivery of reagents. The user initiates the test simply by introducing 30 µl sample into the sample port, and 2 ml water into the fluid reservoir (Fig. 6C). All subsequent operations happen automatically, and a test result appears in the detection zone of the device after ~20 minutes (Fig. 6C).

The operation of this device is first demonstrated using colored dyes (Movie S7 in Supporting Information). 30 µl solutions of yellow food color with 4% trehalose and 0.1% BSA, TBST (Tris buffered saline with 0.1% tween 20), and green food color with 4% trehalose and 0.1% BSA, were dried on legs 1, 2, and 3 respectively (Fig. 6A). Time-lapse images of the device in operation are shown in Fig. 6D with the status of valves tabulated at each time point. Check marks indicate actuated valves. At time, $t = 0$, a 30 µl solution of red food color was introduced into the sample port (Fig. 6D; $t = 10$s). Immediately after this, 2 ml DI water was added into the fluid reservoir (not shown in figure). Addition of water engaged the feeder channel and the timing wick. The feeder channel delivered water to the three legs and rehydrated the dried reagents while red fluid from the sample port continued to flow through the detection strip into the detection zone and the wicking pad (Fig. 6D; $t = 5$ min). None of the four valves had actuated at this point. Valves $V_{ON,1}$ and V_{OFF} actuated at 5.17 and 5.67 min, respectively. Actuation of $V_{ON,1}$ delivered yellow fluid to the detection zone (Fig. 6D; $t = 10$ min). Valves $V_{ON,2}$ and $V_{ON,3}$ actuated at 10 and 15.5 min, delivering wash solution and green fluid, respectively, to the

Lab on a Chip Accepted Manuscript

detection zone (Fig. 6D; t = 14 and 23 min). A montage of time-lapse images of a rectangular region, approximately 4 mm x 4 mm (highlighted by a yellow rectangle in Fig. 6D; t = 23 min), shows sequential delivery of four fluids over the detection zone (Fig. 6E) over 23 minutes.

Finally, we demonstrate a signal amplified ELISA test for P*f*HRP2 on this device. A detailed description of this assay is provided in Fu et al.[23] and in Supporting Information, Section V. The assay follows a standard sandwich format. A murine antibody to P*f*HRP2 was spotted in the detection zone as a capture agent. Another murine antibody to P*f*HRP2 conjugated to gold nanoparticles was used as the labeling agent and dried in leg 1. An anti-mouse antibody was spotted downstream of the capture spot as a control spot. A solution of TBST wash buffer was dried in leg 2 and gold signal enhancement reagents were dried in leg 3. The test was initiated by introducing a 30 µl solution of 5 µg/ml P*f*HRP2 (150 ng total) in fetal bovine serum to the sample port, followed by adding 2 ml DI water to the fluid reservoir. Fig. 6F shows time-lapse images of the detection zone with different reagents flowing over it – no reagent/dry (t = 10 s), sample (t = 5 min), labeling antibody conjugated to gold nanoparticles (t = 10.3 min), wash buffer (t = 16 min), and gold enhancement reagents (t = 23 min). A standard lateral flow assay would have only provided the test result shown at t = 10.3 min (Fig. 6F). This device enables subsequent delivery of wash fluid and gold enhancement reagents, which improves the sensitivity of the assay[23].

There are several advantages of using this device for conducting sequential delivery-based assays. First, the number of pipetting steps is minimized, making it simple for operation by untrained users. The number of user steps in this device is equal to or less than several FDA

Lab on a Chip Accepted Manuscript

approved home test kits, e.g. BinaxNOW® Malaria (Alere, Waltham, MA). Further, the number of fluids delivered sequentially can be increased by increasing the number of legs, without increasing the number of pipetting steps. Second, the volumes delivered through each leg are fully customizable. The same test strip geometry can be used to deliver different volumes of fluids through the legs by changing the size of the legs and the shape of the timing wick. Finally, the performance of this device is robust and reproducible. In the last 6 runs, the CV's in valve actuation time of the four valves on the device were <10% and sequential delivery of the four fluids was successful on all the devices.

The valving toolkit presented here is comprehensive and enables multiple types of automated fluidic operations. One of the salient features of these valves is that they do not introduce any chemicals in the flow path and thus will not affect chemical compatibility of paper microfluidic devices. The use of mechanical actuators and moving paper channels makes these designs more complex compared to paper devices without moving parts. However, fluidic capabilities increase considerably with these valves; capabilities comparable to those achievable in micromachined or PDMS microfluidic devices are imparted to paper microfluidic devices. Even though they may be more complex, they are reasonably easy to construct and involve simply stacking layers of adhesive-backed plastic, PMMA slabs, and paper. Sponge actuators are extremely low cost – the volume amount of sponge required for a 4.5 x 4.5 mm^2 actuator was purchased at a retail cost of ~$0.003 US. Retail cost of all materials and reagents used for the P*f*HRP2 test device was ~$6.8 US, out of which, $4.7 US was the cost of plastic (see Supporting Information, Section VI for a detailed cost analysis). The only machine required to fabricate these parts was a CO_2 laser cutter, which are rapidly becoming cheaper and more accessible. If manufactured in large scale using

Lab on a Chip Accepted Manuscript

injection molding, the cost of plastic parts will reduce to well under a dollar, using a conservative estimate. Thus a device for conducting a multistep ELISA assay can be fabricated for under $3 US. Compared to conventional microfluidic devices, the critical cost saving associated with paper microfluidic devices is the operational cost. Such a paper-based device would not require electricity, batteries, permanent instruments, maintenance, or trained personnel for operation.

Sponge actuators do not spontaneously compress when dried; actuation is irreversible, so these are single-use valves. For most biochemical assays that involve either sequential delivery of fluids to a detection zone, or the controlled movement and incubation of a plug of fluid into different zones of a device, single-use valves work well. The volume of actuating fluid required by these valves can be high. Even though the volume required to expand the actuators is only ~30 µl for time-metered switches, the volume required to wet the glass fiber timing channels is ~500 µl for the longest channel (design E; Fig. 3B). However, as demonstrated in the protein assay device, such large volumes can easily be accommodated in portable test devices. If desired, this volume can be reduced by timing channels made of thinner materials or slower-wetting materials. Before proceeding, it must be ensured that the alternate materials have reproducible flow and a sufficient rate of fluid delivery to the sponge actuators. Another possibility is to use alternate actuators that are not based on fluid absorption. A variety of such alternate strategies may be utilized – the end result should be mechanical motion triggered by the arrival of fluid. Because actuation of these valves is coupled with the arrival of fluid at actuators, they can be used as ‘logic gates’ in paper microfluidic circuits and lay the ground for development of highly integrated paper microfluidic systems.

Lab on a Chip Accepted Manuscript

Experimental

Paper Materials

Plastic-backed and unbacked channels were made of nitrocellulose FF80HP and AE100, respectively (GE Healthcare; Waukesha, WI). Test strip used in the protein detection assay was made of nitrocellulose HF120 (Millipore, Billerica, MA). The adapter channel for volume-metered valves with displaceable metering pads was made of glass fiber grade 691 (VWR, Radnor, PA). All cellulose pads were made of 0.87 mm thick CFSP223000 (Millipore, Billerica, MA), except a 2.7 mm thick cellulose 320 (Ahlstrom, Helsinki, Finland) pad that was used for the volume metering valve with cantilever channel. Glass fiber actuation channels and all glass channels in the protein assay device were made of GR8964 (Ahlstrom). Actuators were made of 2.3 mm thick compressed cellulose sponge #43CC (Sponge Producers Company, St. Louis, MO). All thicknesses reported here are of dry materials.

Device Fabrication

Devices were constructed by stacking layers of 10-mil thick adhesive-backed Mylar (Fralock, Valencia, CA), slabs of poly (methyl methacrylate) (PMMA; McMaster-Carr, Elmhurst, IL), and paper channels. Designs were drawn using DraftSight (Dassault Systemes HQ, France) and all parts were cut using a 42-W CO_2 laser cutter (M360, Universal Laser Systems, Scottsdale, AZ). Individual layers of plastic and paper were cut to desired shapes before stacking. The detailed procedure for cutting nitrocellulose channels was described previously[47]. Compressed sponges were also laser cut to the desired dimensions. The actuator cavity was laser cut in a 2.5 mm thick PMMA layer. Height difference between flow channels was maintained by a 1.5 or 2 mm thick PMMA layer. To create a cantilever channel, laminate protecting the adhesive on a Mylar layer

Lab on a Chip Accepted Manuscript

was selectively removed from under one end of the channel by laser cutting; the other end was not adhered to the surface and was free to move. This movable end of the channel was attached to an impermeable fluid barrier, which was a flap made of 10-mil thick double adhesive backed Mylar. The channel adhered to this flap on its top surface and the bottom surface of the flap adhered over the cavity containing the actuator. There was no adhesive on the bottom surface of the sponge actuator or on the glass fiber actuation channel; good contact between the actuator and the actuation channel was maintained by reducing the width of the actuation channel under the actuator to half, in order to expose the adhesive on the surrounding Mylar. Actuators were adhered on top of actuating channels in this way. Schematics of part-by-part assembly of a device and geometric details of various parts around the actuator are provided in Supporting Information, Section III. Unbacked nitrocellulose channels tended to warp when wet, which resulted in improper contact. To avoid this, unbacked channels were laminated with adhesive-backed 4-mil thick Mylar films at places where they did not make contact with other channels from both sides. For volume-metered valves with displaceable metering pads, the weight and support posts were constructed by stacking three 3.8 mm thick PMMA parts after laser cutting to desired shape.

Experimental Setup, Image Acquisition and Analysis

All devices (except the protein detection device) were set on a 19.1 mm thick black PMMA block with a fluid reservoir etched near one edge. Channel A and timing/actuator channels of all devices extended out into the fluid reservoir. Some valves used different fluids in the actuation and flow channels. For these, the actuation channels extended into a separate cylindrical fluid reservoir attached to the side of the block. The electrode for the electrochemical band marking

Lab on a Chip Accepted Manuscript

system that created pink bands in the yellow fluid (phenol red solution; described by Kauffman et al.[18]) resided on top of channel A just downstream the fluid reservoir. A custom-made humidity chamber with multiple sources of water was used to raise the relative humidity to 75% before addition of fluids into the devices. Images were acquired at intervals of 10 or 15 seconds using a Logitech Pro 9000 (Logitech, Newark, CA) webcam operated using HandyAvi (AZcendant, Tempe, AZ). The location of fluid fronts and pink bands were tracked over time using ImageJ (NIH Research Services Branch). Speed (cm/min) at any instant, *t* (min), was calculated by measuring the distance (cm) traveled by fluid fronts or bands between *t* to *t*+1 min. Volume (µl) passed until time, *t*, was calculated as area under the speed-time curve (cm) from 0 to *t*, multiplied by the width (cm) of the channel and absorption capacity (µl/cm^2) of the channel material. Area under the curve was approximated by the trapezoidal rule. Absorption capacity of nitrocellulose materials was experimentally determined[26] to be 10 µl/cm^2. The protein detection device was run on a tabletop at ambient temperature and humidity to demonstrate its standalone operation.

Protein Detection Assay

See Supporting Information, Section V.

Conclusion

We have, for the first time, demonstrated functional mechanically actuated valves that can be programmed to actuate automatically in paper microfluidics. We also demonstrated the use of these valves in designing portable devices that can be operated by untrained users to conduct complex detection chemistries. These valves are enabling for the two ongoing projects in our

Lab on a Chip Accepted Manuscript

laboratory aimed at developing paper-based diagnostic devices for conducting nucleic acid amplification or protein binding assays. Broadly, this valving and automation toolkit will enable researchers to conduct complex multi-step fluidic operations in paper microfluidic devices while maintaining their fundamental advantage, i.e., fluid flow without pumps and electricity.

Acknowledgments

The work presented in this paper was carried out with support of two grants to PI Paul Yager at the University of Washington: one from DARPA DSO (grant number HR0011-11-2-0007), and one from the National Institute of Allergy and Infectious Disease of the National Institutes of Health (Award Number R01AI096184). We wish to acknowledge helpful communications with collaborators on these grants at UW, Seattle Children's, PATH, GE Global Research, and ELITechGroup North America Inc. Molecular Diagnostics (previously Epoch Biosciences). We would like to thank Tinny Liang, Sujatha Ramachandran, Koji Abe, and Shichu Huang for help with protein assays, and Peter Kauffman for the design of the electrochemical band marking setup. The information in this manuscript does not necessarily reflect the position or policy of the government, and no official endorsement should be inferred. The content is solely the responsibility of the authors and does not necessarily represent the official views of the National Institutes of Health.

Lab on a Chip Accepted Manuscript

References

1. A. W. Martinez, S. T. Phillips, M. J. Butte, and G. M. Whitesides, *Angew. Chem. Int. Ed. Engl.*, 2007, **46**, 1318–1320.

2. A. W. Martinez, S. T. Phillips, G. M. Whitesides, and E. Carrilho, *Anal. Chem.*, 2010, **82**, 3–10.

3. A. K. Yetisen, M. S. Akram, and C. R. Lowe, *Lab Chip*, 2013, **13**, 2210–51.

4. B. Li, W. Zhang, L. Chen, and B. Lin, *Electrophoresis*, 2013, **34**, 2162–8.

5. S. Byrnes, G. Thiessen, and E. Fu, *Bioanalysis*, 2013, **5**, 2821–36.

6. P. Rattanarat, W. Dungchai, D. Cate, J. Volckens, O. Chailapakul, and C. S. Henry, *Anal. Chem.*, 2014, **86**, 3555–3562.

7. S. A. Bhakta, R. Borba, M. Taba, C. D. Garcia, and E. Carrilho, *Anal. Chim. Acta*, 2014, **809**, 117–22.

8. Y. Zhang and D. Rochefort, *Anal. Chim. Acta*, 2013, **800**, 87–94.

9. A. A. Weaver, H. Reiser, T. Barstis, M. Benvenuti, D. Ghosh, M. Hunckler, B. Joy, L. Koenig, K. Raddell, and M. Lieberman, *Anal. Chem.*, 2013, **85**, 6453–60.

10. B. Li, L. Fu, W. Zhang, W. Feng, and L. Chen, *Electrophoresis*, 2014, **35**, 1152–9.

11. L. He, T. Nan, Y. Cui, S. Guo, W. Zhang, R. Zhang, G. Tan, B. Wang, and L. Cui, *Malar. J.*, 2014, **13**, 127.

12. D. Z. Hung, J. H. Lin, J. F. Mo, C. F. Huang, and M. Y. Liau, *Clin. Toxicol. (Phila).*, 2014, **52**, 187–91.

13. Y. K. Oh, H.-A. Joung, S. Kim, and M.-G. Kim, *Lab Chip*, 2013, **13**, 768–72.

14. Z. Fang, C. Ge, W. Zhang, P. Lie, and L. Zeng, *Biosens. Bioelectron.*, 2011, **27**, 192–6.

15. A. W. Martinez, S. T. Phillips, and G. M. Whitesides, *Proc. Natl. Acad. Sci. U. S. A.*, 2008, **105**, 19606–19611.

16. A. W. Martinez, S. T. Phillips, Z. Nie, C.-M. Cheng, E. Carrilho, B. J. Wiley, and G. M. Whitesides, *Lab Chip*, 2010, **10**, 2499–2504.

17. E. Fu, B. Lutz, P. Kauffman, and P. Yager, *Lab Chip*, 2010, **10**, 918–920.

Lab on a Chip Accepted Manuscript

18. P. Kauffman, E. Fu, B. Lutz, and P. Yager, *Lab Chip*, 2010, **10**, 2614–2617.

19. E. Fu, P. Kauffman, B. Lutz, and P. Yager, *Sensors Actuators B. Chem.*, 2010, **149**, 325–328.

20. E. Fu, T. Liang, J. Houghtaling, S. Ramachandran, S. A. Ramsey, B. Lutz, and P. Yager, *Anal. Chem.*, 2011, **83**, 7941–7946.

21. B. R. Lutz, P. Trinh, C. Ball, E. Fu, and P. Yager, *Lab Chip*, 2011, **11**, 4274–4278.

22. E. Fu, S. A. Ramsey, P. Kauffman, B. Lutz, and P. Yager, *Microfluid. Nanofluidics*, 2011, **10**, 29–35.

23. E. Fu, T. Liang, P. Spicar-Mihalic, J. Houghtaling, S. Ramachandran, and P. Yager, *Anal. Chem.*, 2012, **84**, 4574–4579.

24. E. Fu, P. Yager, P. N. Floriano, N. Christodoulides, and J. Mcdevitt, *IEEE Pulse*, 2011, **2**, 40–50.

25. S. Mendez, E. M. Fenton, G. R. Gallegos, D. N. Petsev, S. S. Sibbett, H. a Stone, Y. Zhang, and G. P. López, *Langmuir*, 2010, **26**, 1380–1385.

26. B. J. Toley, B. Mckenzie, T. Liang, J. R. Buser, P. Yager, and E. Fu, *Anal. Chem.*, 2013, **85**, 11545–11552.

27. B. Lutz, T. Liang, E. Fu, S. Ramachandran, P. Kauffman, and P. Yager, *Lab Chip*, 2013, **13**, 2840–7.

28. J. Houghtaling, T. Liang, G. Thiessen, and E. Fu, *Anal. Chem.*, 2013, **85**, 11201–4.

29. S. Jahanshahi-Anbuhi, A. Henry, V. Leung, C. Sicard, K. Pennings, R. Pelton, J. D. Brennan, and C. D. M. Filipe, *Lab Chip*, 2014, **14**, 229–36.

30. H. Noh and S. T. Phillips, *Anal. Chem.*, 2010, **82**, 4181–4187.

31. H. Chen, J. Cogswell, C. Anagnostopoulos, and M. Faghri, *Lab Chip*, 2012, **12**, 2909.

32. R. Gerbers, W. Foellscher, H. Chen, C. Anagnostopoulos, and M. Faghri, *Lab Chip*, 2014, **14**, 4042–9.

33. C. K. W. Koo, F. He, and S. R. Nugen, *Analyst*, 2013, **138**, 4998–5004.

34. X. Li, J. Tian, T. Nguyen, and W. Shen, *Anal. Chem.*, 2008, **80**, 9131–9134.

35. X. Li, P. Zwanenburg, and X. Liu, *Lab Chip*, 2013, **13**, 2609–14.

Lab on a Chip Accepted Manuscript

36. A. C. Glavan, R. V Martinez, E. J. Maxwell, A. B. Subramaniam, R. M. D. Nunes, S. Soh, and G. M. Whitesides, *Lab Chip*, 2013, **13**, 2922–30.

37. X. Li, P. Zwanenburg, and X. Liu, *Lab Chip*, 2013, **13**, 2609–14.

38. N. Kurn, R. D. Patel, M. Becker, and E. F. Ullman, 1992, 1.

39. R. D. Patel, N. Kurn, M. Becker, and E. F. Ullman, 1992.

40. R. A. Bunce, G. H. G. H. Thorpe, J. E. C. Gibbons, L. J. Keen, and M. R. Walker, 1993.

41. D. J. Beebe, J. S. Moore, J. M. Bauer, Q. Yu, R. H. Liu, C. Devadoss, and B. Jo, *Nature*, 2000, **404**, 588–590.

42. D. Eddington and D. J. Beebe, *Adv. Drug Deliv. Rev.*, 2004, **56**, 199–210.

43. E. W. Washburn, *Phys. Rev.*, 1921, **17**, 273–283.

44. R. Lucas, *Kolloid Z*, 1918, **23**.

45. J. . Bell and F. . Cameron, *J. Phys. Chem.*, 1906, **10**, 658–674.

46. J. Li and J. Macdonald, *Biosens. Bioelectron.*, 2015, **64**, 196–211.

47. P. Spicar-Mihalic, B. J. Toley, J. Houghtaling, T. Liang, P. Yager, and E. Fu, *J. Micromechanics Microengineering*, 2013, **23**, 067003.

Lab on a Chip Accepted Manuscript

Figure Captions

Figure 1. The valving and automation toolkit. All valves make use of absorbent expandable elements as actuators. Valves can be broadly classified into two categories – **A**. those that actuate after a fixed period of time and make use of an external fluid for actuation, and **B**. those that actuate after a fixed volume of fluid flow and make use of an internal process fluid for actuation. Time-metered valves consist of **A1**. On-switches that start fluid flow between two channels, **A2**. Off-switches that stop fluid flow between two channels, and **A3**. Diversion-switches that divert fluid flow from one channel to another. Volume-metered valves demonstrated here are diversion switches that use two different mechanisms: **B1**. Moving channels with fixed volume-metering pads, and **B2**. Fixed channels with moving volume-metering pads.

Figure 2. The three types of time-metered valves – on-switch (**A-C**), off-switch (**D-F**), and diversion switch (**G-I**). These valves consist of nitrocellulose flow channels (containing yellow fluid) and glass fiber actuation channels (containing water), separated by an impermeable fluid barrier (see legend). Water is added to the actuation channels manually after a certain period of time to actuate valves. **A**. Schematic of an on-switch. It consists of two flow channels, A and B, placed at two different levels. Upon actuation, one end of channel A is lifted up to connect to one end of channel B. **B**. Images of the on-switch before and after actuation. **C**. Speed of the fluid front in the flow channels as a function of time shows the step increase in the flow speed on valve actuation. **D**. Schematic of an off-switch. It consists of two perpendicular flow channels, A and B, placed on one level and initially connected at one end. Upon actuation, channel A is lifted up to disconnect from channel B. **E**. Images of the off-switch before and after actuation. **F**. Flow rate (linear velocity) as a function of time, as tracked by an electrochemical band marking setup, shows a rapid drop on valve actuation. **G**. Schematic of a diversion switch. It is a combination of an on-switch and an off-switch that diverts fluid flow from channel B to channel C. **H**. Images of the diversion-switch before and after actuation. **I**. Flow rate (linear velocity) as a function of

Lab on a Chip Accepted Manuscript

time shows a sharp drop for channel B and a sharp rise for channel C on valve actuation. All scale bars are 1 cm. In **C**, **F**, and **I**, curves were added to guide the eye.

Figure 3. Programming valve actuation time. **A**. Time-lapse images of an on-switch with a serpentine actuation channel that times valve actuation. Channel A and the actuation channel were connected to a common fluid reservoir. Yellow fluid was added in the reservoir at time, $t = 0$. The fluid reached the end of channel A at 4.3 min. Fluid in the timing/actuation channel reached the actuator at 10 minutes and actuated the valve. Note that the fluid appears darker in the actuation channel because it is thicker than channels A and B. **B**. Time required for fluid to traverse the length of different lengths of serpentine glass fiber channels. Percent values are coefficients of variation (N=6). **C**. Time-lapse images of a device consisting of two on-switches (valve 1 and valve 2; dotted red squares) that actuate sequentially by a common timing/actuation channel. Valves actuated when fluid in the timing channel reached the corresponding actuators.

Figure 4. Volume-metered valve with a cantilever channel. **A**. Schematic of a volume-metered flow-diversion switch. It consists of two channels, A and B, placed at two different heights. Channel A connects to a metering pad placed under it, which delivers fluid to an actuator, through a connector pad. After the passage of a certain volume of fluid, the actuator expands, disconnects channel A from the metering pad and connects it to channel B. **B**. Time-lapse images of the valve. The length of the metering pad and actuator, W, was 1 cm for this design. Before actuation (4 and 57 min), fluid in channel A flowed into the metering pad. After actuation (65 and 79 min), fluid was diverted into channel B. Scale bar is 1 cm. **C**. Linear velocity as a function of time for the device shown in **B** showed a steady flow into the metering pad (solid circles; red line) before actuation. During actuation, the velocity into the metering pad decreased to zero, and after actuation, velocity into channel B (hollow circles; green line) increased from zero to a positive value. **D**. Normalized mean volumes of fluid flow before valves actuated, as a function of W. Percent values are coefficients of variation. Mean volumes of actuation are provided next to the data points (N = 5 for $W = 1$ cm and N = 4 for $W = 0.5$ cm). In **C**, curves are added to guide the eye.

Lab on a Chip Accepted Manuscript

Figure 5. Volume-metered valve with a moveable metering pad. **A**. Schematic of the volume-metered flow-diversion switch showing transverse and lateral views. It consists of a metering pad with actuators inserted in it, resting on top of a flow channel. Actuators extend out of the metering pad into cavities on the surface. Firm contact between the flow channel and metering pad is ensured by a weight attached on top of the pad. Fluid in the channel flows into the metering pad initially, until actuators expand and lift the pad off. After actuation, fluid flows downstream the valve in the flow channel. The lateral view shows the schematic of this valve with two flow channels, A and B, with an adapter channel in between. **B**. Top and side views of the valve before (t = 15 min) and after (t = 38 min) actuation. Fluid flowed into the metering pad before actuation (t = 15 min; top view) and into channel B after actuation (t = 38 min; top view). Scale bar is 1 cm. Side view shows the sponge actuator before (t = 15 min) and after (t = 38 min) actuation. Scale bar is 1 mm. **C**. Flow rates (linear velocity) of fluid flowing into the metering pad (solid circles; red line) and channel B (hollow circles; green line) as a function of time. Graphs show steady flow into the metering pad and channel B, before and after actuation, respectively. There was slight leakage of fluid into channel B before actuation, between t = 18 and 25 min (dotted rectangle).

Figure 6. Protein detection device. **A**. Top view of the device showing important parts. The device consists of one nitrocellulose test strip, and three source legs, one feeder channel, and one timing wick, all made of glass fiber. There are three on-switches, $V_{ON,1}$, $V_{ON,2}$, $V_{ON,3}$, between the test strip and source legs 1, 2, and 3, respectively, and an off-switch, V_{OFF}, that, when actuated, disconnects the feeder channel from all three source legs. Scale bar is 1 cm. **B**. The shape of the glass fiber timing wick and the location of the four valves. The wick splits at the point indicated by the green asterisk – one branch actuates V_{OFF} and the other actuates the three on-switches sequentially. **C**. Schematic of a step-by-step procedure of conducting the protein detection test. The test is initiated by adding 30 µl sample in the sample inlet port and 2 ml water in the fluid reservoir. No further user steps are required and the result can be read in the detection zone after 20 minutes. **D**. The operation of the device is demonstrated using colored fluids. Time-lapse images show the sequential flow over the detection zone of i) red fluid introduced through the

Lab on a Chip Accepted Manuscript

sample port (t = 5 min), ii) yellow fluid (t = 10 min), iii) a wash fluid (t = 14 min), and iv) green fluid (t = 23 min), rehydrated from legs 1, 2, and 3, respectively. The status of valves is tabulated at each time point; a green check indicates an actuated valve. Scale bar is 1 cm. **E**. Montage of time-lapse images over a square region indicated by the yellow box (t = 23 min) in the detection zone. **F**. Time-lapse images of the detection zone of the device that was used to conduct a P*f*HRP2 protein detection assay. The two spots represent test result (bottom) and control (top). The sample flows over the detection zone first (t = 5 min), followed by the labeling antibody (t = 10.3 min), wash buffer (t = 16 min), and gold enhancement reagents (t = 23 min).

Lab on a Chip Accepted Manuscript

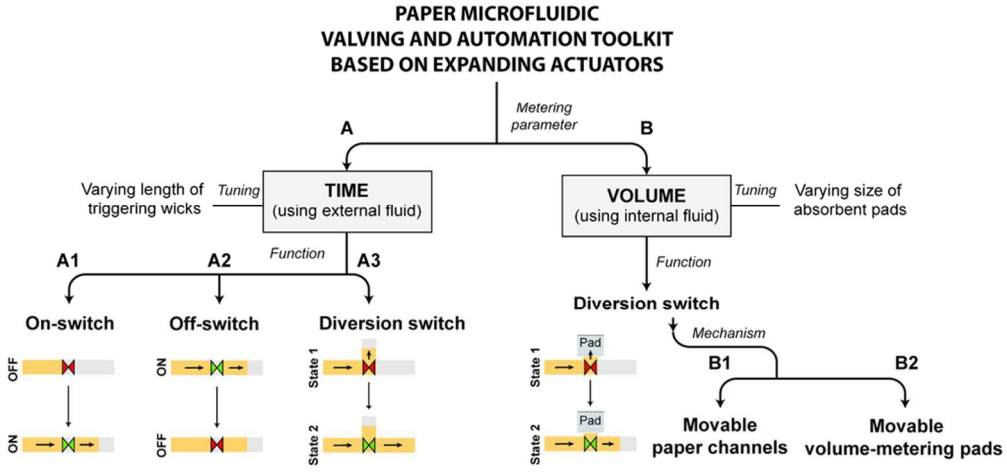

Figure 1. The valving and automation toolkit. All valves make use of absorbent expandable elements as actuators. Valves can be broadly classified into two categories – A. those that actuate after a fixed period of time and make use of an external fluid for actuation, and B. those that actuate after a fixed volume of fluid flow and make use of an internal process fluid for actuation. Time-metered valves consist of A1. On-switches that start fluid flow between two channels, A2. Off-switches that stop fluid flow between two channels, and A3. Diversion-switches that divert fluid flow from one channel to another. Volume-metered valves demonstrated here are diversion switches that use two different mechanisms: B1. Moving channels with fixed volume-metering pads, and B2. Fixed channels with moving volume-metering pads.
86x43mm (300 x 300 DPI)

Lab on a Chip Accepted Manuscript

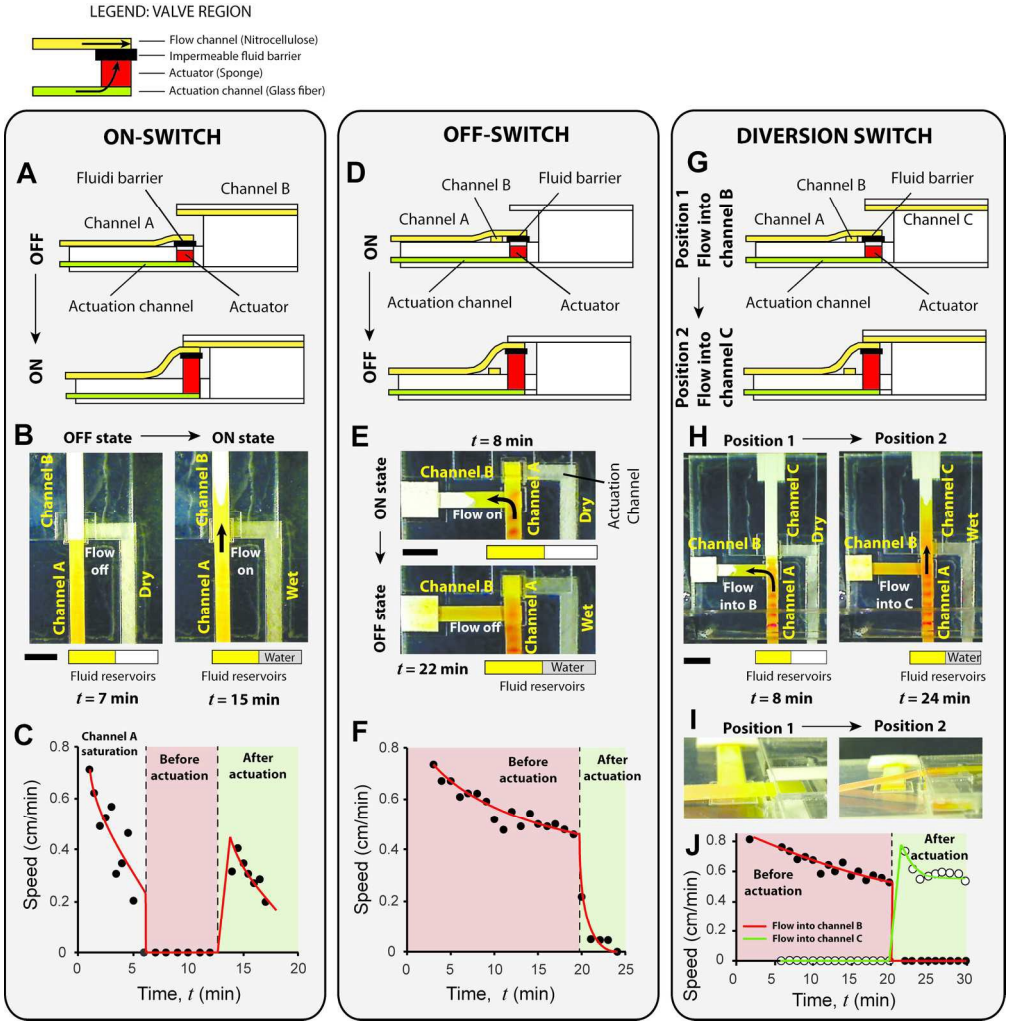

Figure 2. The three types of time-metered valves – on-switch (A-C), off-switch (D-F), and diversion switch (G-I). These valves consist of nitrocellulose flow channels (containing yellow fluid) and glass fiber actuation channels (containing water), separated by an impermeable fluid barrier (see legend). Water is added to the actuation channels manually after a certain period of time to actuate valves. A. Schematic of an on-switch. It consists of two flow channels, A and B, placed at two different levels. Upon actuation, one end of channel A is lifted up to connect to one end of channel B. B. Images of the on-switch before and after actuation. C. Speed of the fluid front in the flow channels as a function of time shows the step increase in the flow speed on valve actuation. D. Schematic of an off-switch. It consists of two perpendicular flow channels, A and B, placed on one level and initially connected at one end. Upon actuation, channel A is lifted up to disconnect from channel B. E. Images of the off-switch before and after actuation. F. Flow rate (linear velocity) as a function of time, as tracked by an electrochemical band marking setup, shows a rapid drop on valve actuation. G. Schematic of a diversion switch. It is a combination of an on-switch and an off-switch that diverts fluid flow from channel B to channel C. H. Images of the diversion-switch before and after actuation. I. Flow rate (linear velocity) as a function of time shows a sharp drop for channel B and a sharp rise for channel C on valve actuation. All scale bars are 1 cm. In C, F, and I, curves were added to guide the eye.
172x175mm (300 x 300 DPI)

Lab on a Chip Accepted Manuscript

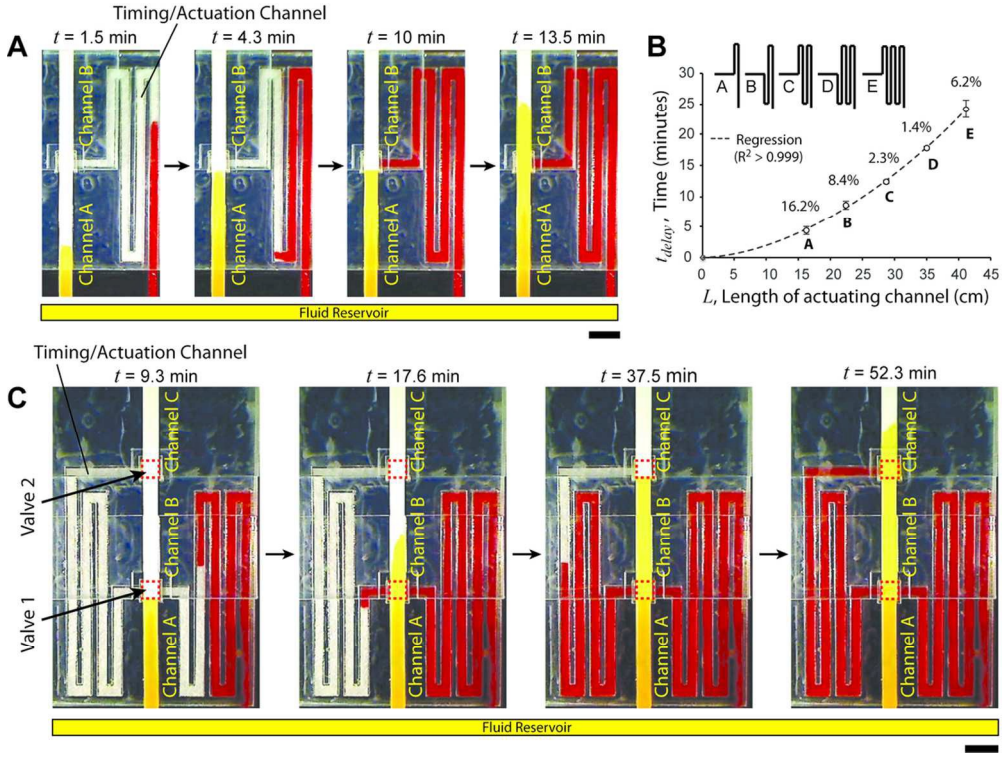

Figure 3. Programming valve actuation time. A. Time-lapse images of an on-switch with a serpentine actuation channel that times valve actuation. Channel A and the actuation channel were connected to a common fluid reservoir. Yellow fluid was added in the reservoir at time, t = 0. The fluid reached the end of channel A at 4.3 min. Fluid in the timing/actuation channel reached the actuator at 10 minutes and actuated the valve. Note that the fluid appears darker in the actuation channel because it is thicker than channels A and B. B. Time required for fluid to traverse the length of different lengths of serpentine glass fiber channels. Percent values are coefficients of variation (N=6). C. Time-lapse images of a device consisting of two on-switches (valve 1 and valve 2; dotted red squares) that actuate sequentially by a common timing/actuation channel. Valves actuated when fluid in the timing channel reached the corresponding actuators.
109x81mm (300 x 300 DPI)

Lab on a Chip Accepted Manuscript

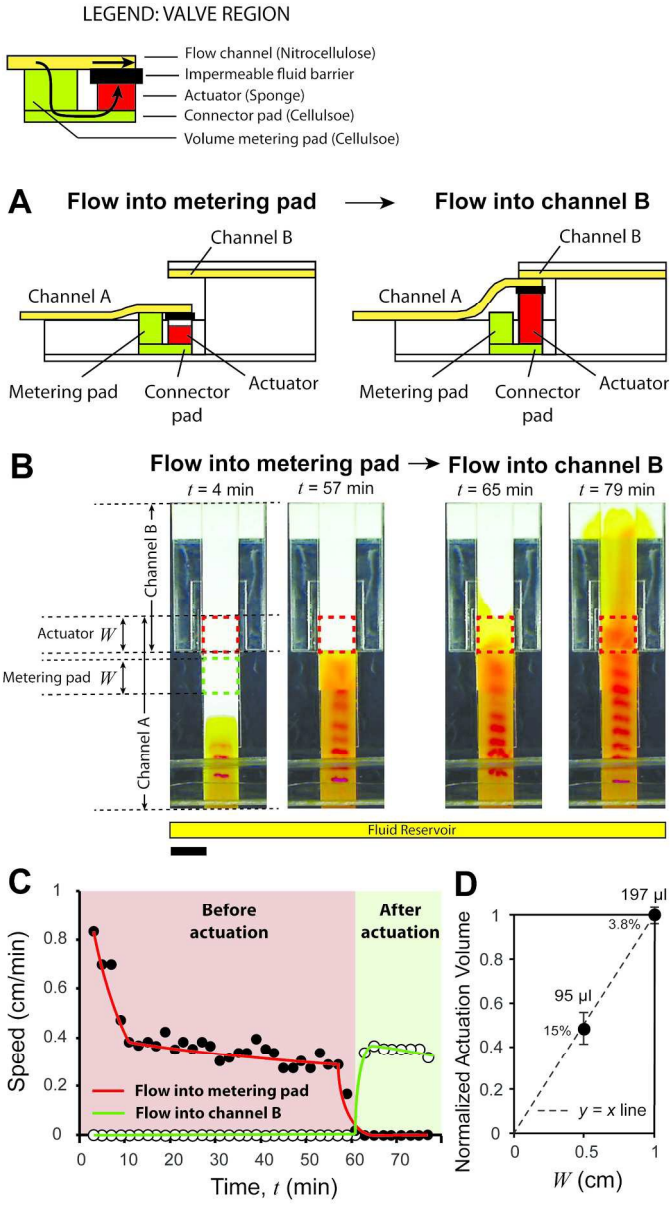

Figure 4. Volume-metered valve with a cantilever channel. A. Schematic of a volume-metered flow-diversion switch. It consists of two channels, A and B, placed at two different heights. Channel A connects to a metering pad placed under it, which delivers fluid to an actuator, through a connector pad. After the passage of a certain volume of fluid, the actuator expands, disconnects channel A from the metering pad and connects it to channel B. B. Time-lapse images of the valve. The length of the metering pad and actuator, W, was 1 cm for this design. Before actuation (4 and 57 min), fluid in channel A flowed into the metering pad. After actuation (65 and 79 min), fluid was diverted into channel B. Scale bar is 1 cm. C. Linear velocity as a function of time for the device shown in B showed a steady flow into the metering pad (solid circles; red line) before actuation. During actuation, the velocity into the metering pad decreased to zero, and after actuation, velocity into channel B (hollow circles; green line) increased from zero to a positive value. D. Normalized mean volumes of fluid flow before valves actuated, as a function of W. Percent values are coefficients of variation. Mean volumes of actuation are provided next to the data points (N = 5 for W = 1 cm and N = 4 for W = 0.5 cm). In C, curves are added to guide the eye.

Lab on a Chip Accepted Manuscript

148x262mm (300 x 300 DPI)

Lab on a Chip Accepted Manuscript

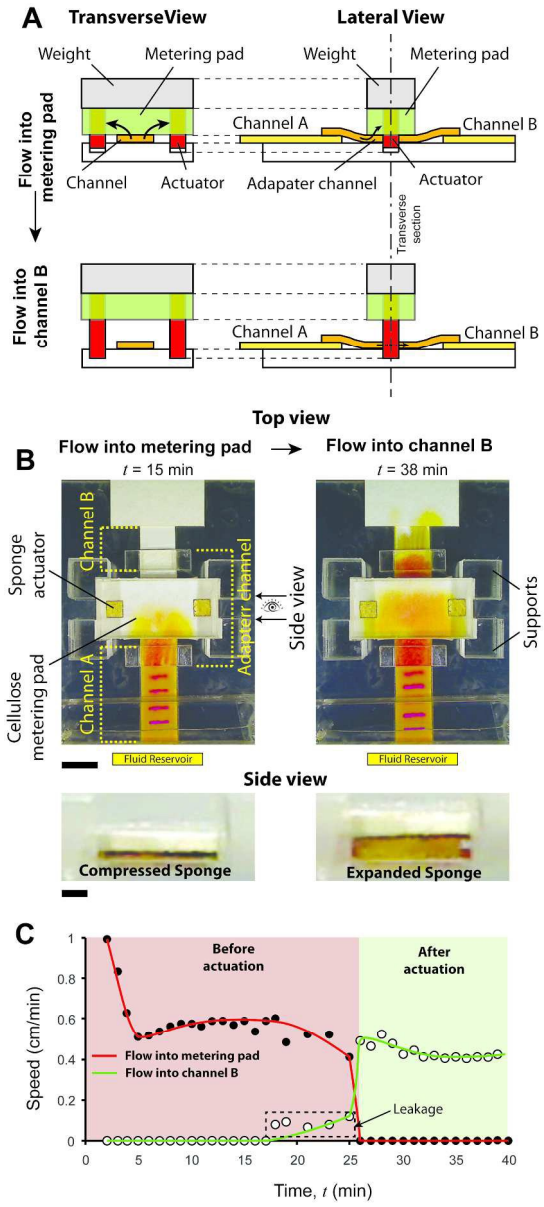

Figure 5. Volume-metered valve with a moveable metering pad. A. Schematic of the volume-metered flow-diversion switch showing transverse and lateral views. It consists of a metering pad with actuators inserted in it, resting on top of a flow channel. Actuators extend out of the metering pad into cavities on the surface. Firm contact between the flow channel and metering pad is ensured by a weight attached on top of the pad. Fluid in the channel flows into the metering pad initially, until actuators expand and lift the pad off. After actuation, fluid flows downstream the valve in the flow channel. The lateral view shows the schematic of this valve with two flow channels, A and B, with an adapter channel in between. B. Top and side views of the valve before (t = 15 min) and after (t = 38 min) actuation. Fluid flowed into the metering pad before actuation (t = 15 min; top view) and into channel B after actuation (t = 38 min; top view). Scale bar is 1 cm. Side view shows the sponge actuator before (t = 15 min) and after (t = 38 min) actuation. Scale bar is 1 mm. C. Flow rates (linear velocity) of fluid flowing into the metering pad (solid circles; red line) and channel B (hollow circles; green line) as a function of time. Graphs show steady flow into the metering pad and channel B, before and after actuation, respectively. There was slight leakage of fluid into channel B

Lab on a Chip Accepted Manuscript

before actuation, between t = 18 and 25 min (dotted rectangle).
192x428mm (300 x 300 DPI)

Lab on a Chip Accepted Manuscript

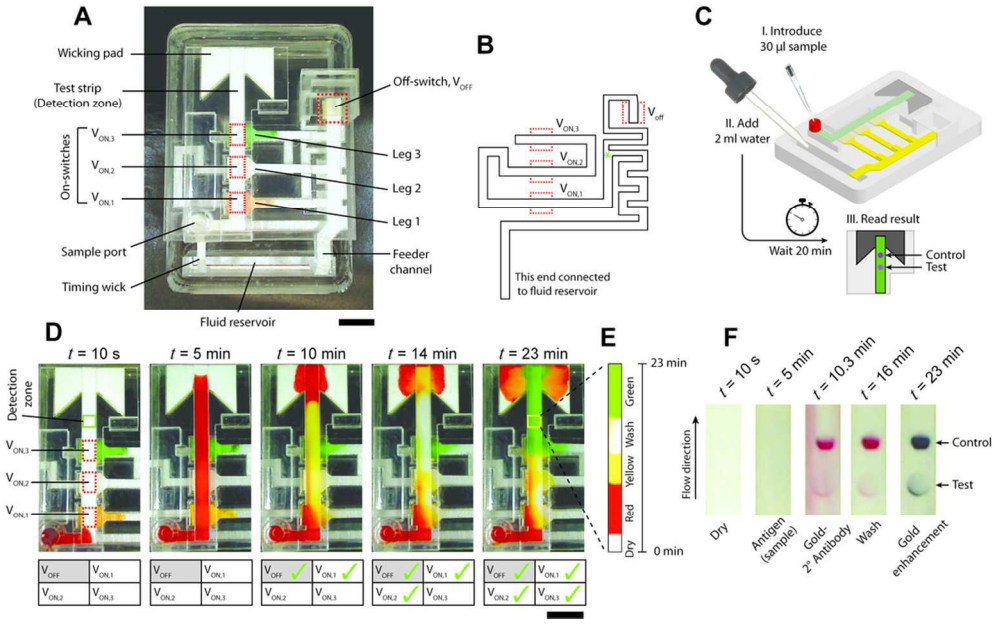

Figure 6. Protein detection device. A. Top view of the device showing important parts. The device consists of one nitrocellulose test strip, and three source legs, one feeder channel, and one timing wick, all made of glass fiber. There are three on-switches, VON,1, VON,2, VON,3, between the test strip and source legs 1, 2, and 3, respectively, and an off-switch, VOFF, that, when actuated, disconnects the feeder channel from all three source legs. Scale bar is 1 cm. B. The shape of the glass fiber timing wick and the location of the four valves. The wick splits at the point indicated by the green asterisk – one branch actuates VOFF and the other actuates the three on-switches sequentially. C. Schematic of a step-by-step procedure of conducting the protein detection test. The test is initiated by adding 30 µl sample in the sample inlet port and 2 ml water in the fluid reservoir. No further user steps are required and the result can be read in the detection zone after 20 minutes. D. The operation of the device is demonstrated using colored fluids. Time-lapse images show the sequential flow over the detection zone of i) red fluid introduced through the sample port (t = 5 min), ii) yellow fluid (t = 10 min), iii) a wash fluid (t = 14 min), and iv) green fluid (t = 23 min), rehydrated from legs 1, 2, and 3, respectively. The status of valves is tabulated at each time point; a green check indicates an actuated valve. Scale bar is 1 cm. E. Montage of time-lapse images over a square region indicated by the yellow box (t = 23 min) in the detection zone. F. Time-lapse images of the detection zone of the device that was used to conduct a PfHRP2 protein detection assay. The two spots represent test result (bottom) and control (top). The sample flows over the detection zone first (t = 5 min), followed by the labeling antibody (t = 10.3 min), wash buffer (t = 16 min), and gold enhancement reagents (t = 23 min).
102x62mm (300 x 300 DPI)

Lab on a Chip Accepted Manuscript